Journal of Experimental Botany, Vol. 58, No. 8, pp. 2225–2236, 2007
doi:10.1093/jxb/erm083 Advance Access publication 24 May, 2007

Journal of Experimental Botany
www.jxb.oxfordjournals.org

RESEARCH PAPER

Conformation of cytoskeletal elements during the division of infected *Lupinus albus* L. nodule cells

Elena E. Fedorova[1,2], María R. de Felipe[1], José J. Pueyo[1] and M. Mercedes Lucas[1,*]

[1] *Instituto de Recursos Naturales, Centro de Ciencias Medioambientales, CSIC, Serrano 115-bis, E-28006 Madrid, Spain*

[2] *K. A. Timiryazev Institute of Plant Physiology RAS, Botanicheskaya 35, Moscow 127276, Russia*

Received 20 December 2006; Revised 5 March 2007; Accepted 20 March 2007

Abstract

Lupin nodule cells maintain their ability to divide for several cycles after being infected by endosymbiotic rhizobia. The conformation of the cytoskeletal elements of nodule cells was studied by fluorescence labelling, immunocytochemistry, and laser confocal and transmission electron microscopy. The dividing infected cells showed the normal microtubule and actin patterns of dividing plant cells. The clustered symbiosomes were tethered to the spindle-pole regions and moved to the cell poles during spindle elongation. In metaphase, anaphase, and early telophase, the symbiosomes were found at opposite cell poles where they did not interfere with the spindle filaments or phragmoplast. This symbiosome positioning was comparable with that of the organelles (which ensures organelle inheritance during plant cell mitosis). Tubulin microtubules and actin microfilaments appeared to be in contact with the symbiosomes. The possible presence of actin molecular motor myosin in nodules was analysed using a monoclonal antibody against the myosin light chain. The antigen was detected in protein extracts of nodule and root cytosol as bands of approximately 20 kDa (the size expected). In the nodules, an additional polypeptide of 65 kDa was found. Immunogold techniques revealed the antigen to be localized over thin microfilaments linked to the cell wall, as well as over the thicker microfilament bundles and surrounding the symbiosomes. The pattern of cytoskeleton rearrangement in dividing infected cells, along with the presence of myosin antigen, suggests that the positioning of symbiosomes in lupin nodule cells might depend on the same mechanisms used to partition genuine plant cell organelles during mitosis.

Key words: Actin, bacteroid, *Bradyrhizobium*, lupin, myosin, organelle, *Rhizobium*, symbiosome, tubulin.

Introduction

The cytoskeletal network, which is composed of microtubules and actin microfilaments, co-ordinates a number of cell activities including cell division, cell shape change, intracellular transport, and cell differentiation. The cytoskeleton also spatially organizes the organelles and serves as a scaffold for their movement (Hashimoto, 2003; Wasteneys and Galway, 2003). The actin cytoskeleton and its associated elements provide key targets in many plant signalling events, and also transduce signal information (Drøbak *et al*., 2003). Moreover, the plant cytoskeleton plays an important role in mediating the cell response to pathogens and symbionts (Takemoto and Hardham, 2004).

During the establishment and function of endosymbiosis between legumes and nodulating bacteria, the activities of the plant cell notably change to create an environment favourable for these nitrogen-fixing bacteria. The functions of the eukaryote cytoskeleton with respect to the prokaryotes that live and propagate inside infected cells are not completely clear, but the cytoskeleton seems to reorganize after infection. The rearrangement of cytoskeletal elements has been described in root hairs during the early stages of infection (Cárdenas *et al*., 1988, 2003; Allen *et al*., 1994; Timmers *et al*., 1999; Lhuissier *et al*., 2001; Weeransinghe *et al*., 2003; Sieberer *et al*., 2005; Vassileva *et al*., 2005), and their disorganization in freshly infected cells has been reported in indeterminate nodules of *Medicago sativa* (Timmers *et al*., 1998) and *Pisum sativum* (Davidson and Newcomb, 2001*a*, *b*). In alfalfa

* To whom correspondence should be addressed: E-mail: mlucas@ccma.csic.es

nodules, a progressive disorganization of the endoplasmic and cortical microtubules has been reported in the layers of the pre-fixing zone during cell differentiation, while the cortical cytoskeleton is re-established in pre-fixing cells adjacent to the nitrogen-fixing zone (Timmers *et al*., 1998). Cytoskeletal disorganization, with a gradient from the outer meristematic cells to the more central cells, has been recorded in developing determinate nodules of *Macroptilium atropurpureum* (Timmers *et al*., 1998). Changes in the actin filament and microtubular configuration have also been reported in mature infected cells of *M. atropurpureum*. In the determinate nodules of *Glycine max*, the cytoplasmic array of actin microfilaments in mature infected cells is denser than in uninfected cells or incipient nodules, and forms a honeycomb pattern (Whitehead *et al*., 1998).

In all the above-mentioned legumes, bacteria invade the plant through the so-called infection thread, a tubular structure that forms in the root hair. Bacteria are released into the host cell cytoplasm from this structure, surrounded by a plant-derived peribacteroid membrane (PBM). At this stage, the bacteria are referred to as bacteroids and the bacteroid–PBM unit as the symbiosome. In most of the legume nodules studied, host cells lose their ability to divide once they become infected. In typical indeterminate nodules (*Pisum*, *Medicago*, and *Trifolium*) some cells of the meristem cease to divide and become invaded by bacteria released from the infection threads (Brewin, 1991). Some authors suggest that in nodules with determinate meristems (*Glycine*, *Phaseolus*, and *Lotus*), young infected cells can maintain their meristematic activity, although the division process is not sustained for long (Patriarca *et al*., 2004).

Lupinus albus, a widely cultivated temperate legume, establishes a symbiotic relationship with slow-growing *Bradyrhizobium* sp. (*Lupinus*). Lupin root nodules are recognized as a unique subtype of indeterminate nodules: lupinoid nodules (Bergersen, 1982). These do not show the characteristic developmental zonation of elongated indeterminate nodules, but share certain features with spherical determinate nodules. Similar to the determinate nodules of *Phaseolus vulgaris* (Patriarca *et al*., 1996), the youngest infected cells in lupin nodules are situated in basolateral regions and the oldest in the middle part of the nodule.

Recently, the early steps of white lupin nodulation have been described in detail (González-Sama *et al*., 2004). Root infection and host cell invasion do not occur via real infection threads in white lupin nodules. Rhizobia penetrate intercellularly, invading a subepidermal cortical cell via structurally altered regions of its cell wall. The development of the infection in lupinoid nodules proceeds by the repeated division of already infected cells (Tang *et al*., 1993; González-Sama *et al*., 2004). Infected cell division had also been reported in nodules of *Arachis hypogea* (Chandler, 1978), *Stylosanthes* spp. (Chandler *et al*., 1982), *Sarothamnus scoparius* (Sajnaga *et al*., 2001), and *Genista tinctoria* (Kalita *et al*., 2006), none of which has infection threads.

Endosymbiotic rhizobia act as plant organelles in terms of nitrogen metabolism (Lodwig *et al*., 2003). Using the infected cell as a new ecological niche, rhizobia proliferate rapidly and bacteroids promptly fill it. Plastids and mitochondria—'ancient' microsymbionts (Douglas, 1998; Gray *et al*., 1999)—also have the ability to divide in the cytoplasm. Their movement and distribution within cells is highly regulated, and elements of the cytoskeleton are involved in the correct partitioning of these organelles between the daughter cells during cytokinesis (King, 2002; Sheahan *et al*., 2004). Microtubules with kinesins and dineins as molecular motors plus the actin–myosin complex are involved in the intracellular transport of subcellular organelles and secure their equal distribution between daughter cells (Warren and Wickner, 1996). The ability of cells to take up micro-organisms gave rise to the evolution of mitochondria and plastid-bearing plant cells, and the intracellular accommodation of root nodule symbionts may involve similar strategies (Parniske, 2000). The sustained ability of host cells to divide despite the presence of multiplying bacteria in the cytoplasm makes infected cells of *L. albus* a good model in which to study the processes of plant cell division and the segregation of symbiosomes during cytokinesis.

The role of the different cytoskeleton elements and their associated proteins in the movement, positioning, and segregation of symbiosomes in the host cell remains to be clarified, and nothing is known about the exact localization or role of actin molecular motor myosin in infected legume nodule cells. The aim of the present work was to investigate cytoskeleton dynamics in different cell types of *L. albus* nodules, with particular emphasis on dividing infected cells. The conformation of tubulin and actin elements and the localization of the myosin light chain were analysed to determine their involvement in symbiosome distribution and segregation. To our knowledge, this is the first study of cytoskeletal element rearrangement during the division of infected symbiotic cells.

Materials and methods

Plant material

Lupinus albus L. cv. Multolupa plants were inoculated 3 d after sowing with *Bradyrhizobium* sp. (*Lupinus*) strain ISLU16, and grown as previously described (González-Sama *et al*., 2006). Nodules were collected 12–25 d after sowing.

Light microscopy

Nodule samples were fixed and embedded in LR White resin (London Resin Co.) and polymerized at 60 °C as described by Fedorova *et al*. (1999). Semi-thin sections (1 μm) were cut with

a Reichert Ultracut S ultramicrotome and stained with methylene blue for direct observation using a Zeiss Axiophot photomicroscope.

Immunolocalization of microtubules

Nodules were hand cut into 70–150 μm thick sections with a double-edged razor blade. Sections were fixed for 1 h in 4% freshly depolymerized paraformaldehyde in microtubule stabilizing buffer containing 60 mM PIPES, 10 mM EGTA, 1 mM $MgCl_2$, 0.3% Triton X-100, 10% dimethylsulphoxide (DMSO), pH 6.9 (Timmers *et al*., 1998), and post-fixed in 4% paraformaldehyde in phosphate-buffered saline (PBS) pH 7.4 for 30 min. Nodule sections were blocked in 3% bovine serum albumin (BSA) and further incubated with the primary antibody (monoclonal anti-tubulin Ab, Sigma) (1:200) for 2 h at 37 °C in PBS containing 0.1% Triton X-100. Anti-mouse IgG-Alexa 488 (Molecular Probes) was used as the secondary antibody (diluted 1:250 in PBS); incubation was allowed to proceed for 2 h at room temperature. Control experiments were performed in the absence of primary antibodies. Sections were counterstained with the DNA stain propidium iodide (10 μM), embedded in Fluoromount G (Electron Microscopy Sciences), and examined using a Leits DM IRB inverted epifluorescence microscope connected to a Leica TCS 4D confocal system.

Actin fluorescent labelling

Actin was labelled with Bodipy Pallacidin FL (Molecular Probes). Nodule sections were incubated (for 2 h at room temperature and in darkness) in phosphate buffer pH 7.2 with 200 μM MBS (3-maleimidobenzoic acid *N*-hydroxysuccinimide ester, Sigma), 0.05% Triton X-100, and Bodipy Pallacidin FL (diluted 1:100). Sections were counterstained, embedded, and examined as described above.

Symbiosome isolation

Microsymbionts were isolated from nodules by fractionation using sucrose cushions in microcentrifuge tubes, as described by Brewin *et al*. (1985) with the following modifications. A 5 g aliquot of nodule was ground on ice in a mortar in the presence of 5 ml of extraction buffer [50 mM HEPES, pH 8.2, 1 mM dithiothteitol (DTT), 5 mM mercaptoethanol, 4 mM EDTA, 1 mM $MgCl_2$, 1 μl ml^{-1} Sigma protease inhibitor cocktail), and 5 ml of polyvinylpolypyrrolidone (PVPP). Symbiosomes were isolated from the homogenized tissue using a sucrose gradient (0.44 mM–1 M–1.5 M). After sonication, the bacteroid fraction was ground in a mortar with liquid nitrogen and centrifuged at 13 000 *g* for 10 min.

SDS-PAGE and immunoblot analysis

Proteins from the bacteroids, nodule, and root cytosol (extracted as described above) were subjected to SDS-PAGE on 8% acrylamide gels in a Laemmli buffer system, and then electrotransferred onto a nitrocellulose membrane (Bio-Rad Trans-Blot nitrocellulose, Bio-Rad). An anti-myosin light chain monoclonal antibody (Sigma) was used as the primary antibody at a dilution of 1:1000. Alkaline phosphatase-conjugated goat anti-mouse IgG (Sigma) was used as the secondary antibody at a dilution of 1:20 000. The reaction was detected colorimetrically (NBT/BCIP, Sigma) according to the standard protocol.

The specificity of the antibody was analysed by its depletion with the light chain of animal myosin (Sigma). This protein, diluted in TRIS-buffered saline (TBS; 0.5 μg $μl^{-1}$), was dotted onto nitrocellulose membranes (0.45 μm; Bio-Rad, Trans-blot transfer medium) and incubated for 30 min in blocking solution (2% BSA in TBS) followed by overnight incubation with the anti-myosin monoclonal antibody. The antibody was then removed and reused twice as above, employing new dots of myosin light chain. Each time, the immunoreaction was checked using the secondary antibody and by following the colorimetric reaction as above. Once the depleted antibody did not immunoreact with the dots, it was used in western blotting. The samples loaded onto the gel included extracts of roots, nodules, and pure myosin light chain.

Myosin immunolocalization

Nodules pre-fixed in 1% paraformaldehyde for 30 min at room temperature were hand cut with a razor blade. Sections were treated with 1% mercaptoethanol and 0.1% SDS for 2 min, washed in PBS, and blocked in 3% BSA–PBS for 1 h at room temperature. Sections were incubated overnight at 4 °C with the primary antibody. A monoclonal anti-myosin light chain (Sigma) antibody was used as the primary antibody at a dilution of 1:100. Goat anti-mouse Alexa 488-labelled IgG (Molecular Probes) was used as the secondary antibody (dilution 1:100). Control experiments were performed in the absence of primary antibodies. Sections were counterstained, embedded, and examined as above.

For electron microscopy, nodules were fixed in 1% paraformaldehyde in 50 mM phosphate buffer, embedded in LR white resin, and polymerized with UV light at –20 °C (Fedorova *et al*., 1999). Thin sections (60 nm) were cut using a Leica Reichert Ultracut S microtome. After placing these on nickel grids they were immersed in 1% mercaptoethanol and 0.1% SDS for 2 min, washed twice in PBS, and blocked in 3% BSA in PBS. They were then incubated overnight at 4 °C with the primary antibody (dilution 1:40). Gold-labelled (15 nm) goat anti-mouse antibody (BioCell) was used as the secondary antibody (dilution 1:50; incubation proceeded for 1 h at room temperature). Sections were contrasted with 2% aqueous uranyl acetate and lead citrate, and examined using a STEM LEO 910 electron microscope equipped with a Gatan Bioscan 792 digital camera. To obtain material with better preserved ultrastructure, some nodules were fixed in 4% paraformaldehyde and 5% glutaraldehyde in phosphate buffer (a conventional procedure), post-fixed in 1% OsO_4, and embedded in LR White resin at 60 °C.

Results

In *L. albus* nodules, the infected zone originates from the division of a single infected outer cortical cell (Gonzalez-Sama *et al*., 2004). The primordial nodule consists of a central meristematic zone composed of infected and uninfected cells, surrounded by several layers of cortical cells (Fig. 1A). As the nodule matures [25 d post-infection (dpi)], cell division ceases in the central zone, which includes no uninfected interstitial cells (unlike that seen in other nodule types), and meristematic activity is restricted to the basolateral regions (Fedorova *et al*., 2005). Both in the nodule primordia and in the lateral meristematic zone of young nodules, infected cells at all stages of mitosis were observed (Fig. 1B–F). Symbiosomes accumulated behind the forming nuclei in the highly vacuolated dividing cells, while they appeared randomly orientated and close to the cell walls in interphase cells.

The cytoskeleton in interphase cells

Propidium iodide counterstaining of the nodule sections distinguished the bacteria (red fluorescence) from the

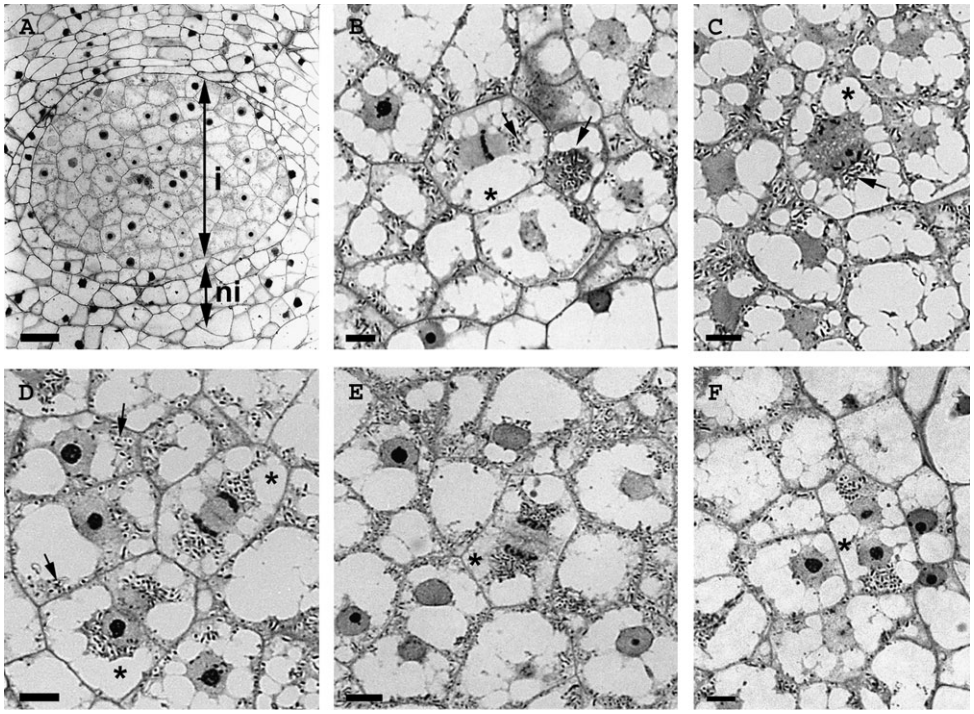

Fig. 1. Dividing infected *Lupinus albus* nodule cells. (A) Nodule (12 dpi) showing dividing infected (i) and uninfected (ni) cells. (B–F) Mitotic images (asterisk) of infected cells in lupin nodules (12–25 dpi): metaphase (B), anaphase (C), telophase (D, E), and freshly divided cells (F). Note that during mitosis the symbiosomes (arrows) are located behind the forming nuclei and move to the cell cortex after cytokinesis. Bars A=75 μm; B–F=10 μm.

cytoskeleton elements (green fluorescence) in laser confocal microscopy.

In the uninfected cortical cells of the lupin nodules, green-labelled microtubules appeared in parallel bundles aligned perpendicularly to the long axis of the cell (Fig. 2A). During plant cell elongation, cortical microtubules are usually arranged in parallel arrays and are predominantly orientated at right angles to the axis of expansion (Wasteneys, 2002). Microtubule distribution in the infected cells was different from that observed in uninfected cells. In the former, the microtubules formed an extensive network of filaments going in all directions, indicating these cells to be undergoing isodiametric growth (Fig. 2B–G). In freshly infected cells housing few symbiosomes, the cortical microtubules were arranged in short, thick bundles (Fig. 2B). In mature infected cells densely packed with symbiosomes, both long cortical bundles of microtubules and randomly organized endoplasmic microtubules were seen (Fig. 2C–F). The cytoplasmic and cortical microtubules bent and criss-crossed, and made contact with the symbiosomes (Fig. 2F). A perinuclear endoplasmic array was also observed in infected cells (Fig. 2C, D).

The cortical cells showed a dense network of actin microfilament bundles encasing the nucleus (Fig. 2H). A network of thin, wavy microfilaments was observed throughout the cytosol of infected cells, continuous with the cell wall region where thick microfilament bundles were observed near the plasmalemma (Fig. 2I). Actin microfilaments were also found enveloping the nucleus; these appeared to be continuous with cytoplasmic actin microfilaments (Fig. 2I). The symbiosomes appeared to be in contact with these actin microfilaments (Fig. 2J).

The cytoskeleton in dividing infected cells

The pattern of microtubule rearrangements during the division of young infected cells was similar to that seen in plant cells undergoing mitosis. Figure 3A–G shows the microtubule arrays in different stages of the division of infected cells. The metaphase spindle, with its dispersed polar region, was fluorescently labelled (Fig. 3A). During metaphase, the cortical microtubules were mostly dissolved and the endoplasmic microtubules appeared as short strands or small dots (Fig. 3A, B). At this stage, when the spindle forms and chromosome segregation occurs in the equatorial region, the symbiosomes were mostly situated towards the poles (Fig. 3A). During anaphase, the microtubules expanded centrifugally, driving the chromosomes to the opposite poles of the cell; at this time, the symbiosomes were located in the lateral regions of the spindle and at the poles, but not in the division plane (Fig. 3C, D). At the anaphase–telophase transition, the phragmoplast appeared as a concentrated cylinder of microtubules between the daughter nuclei

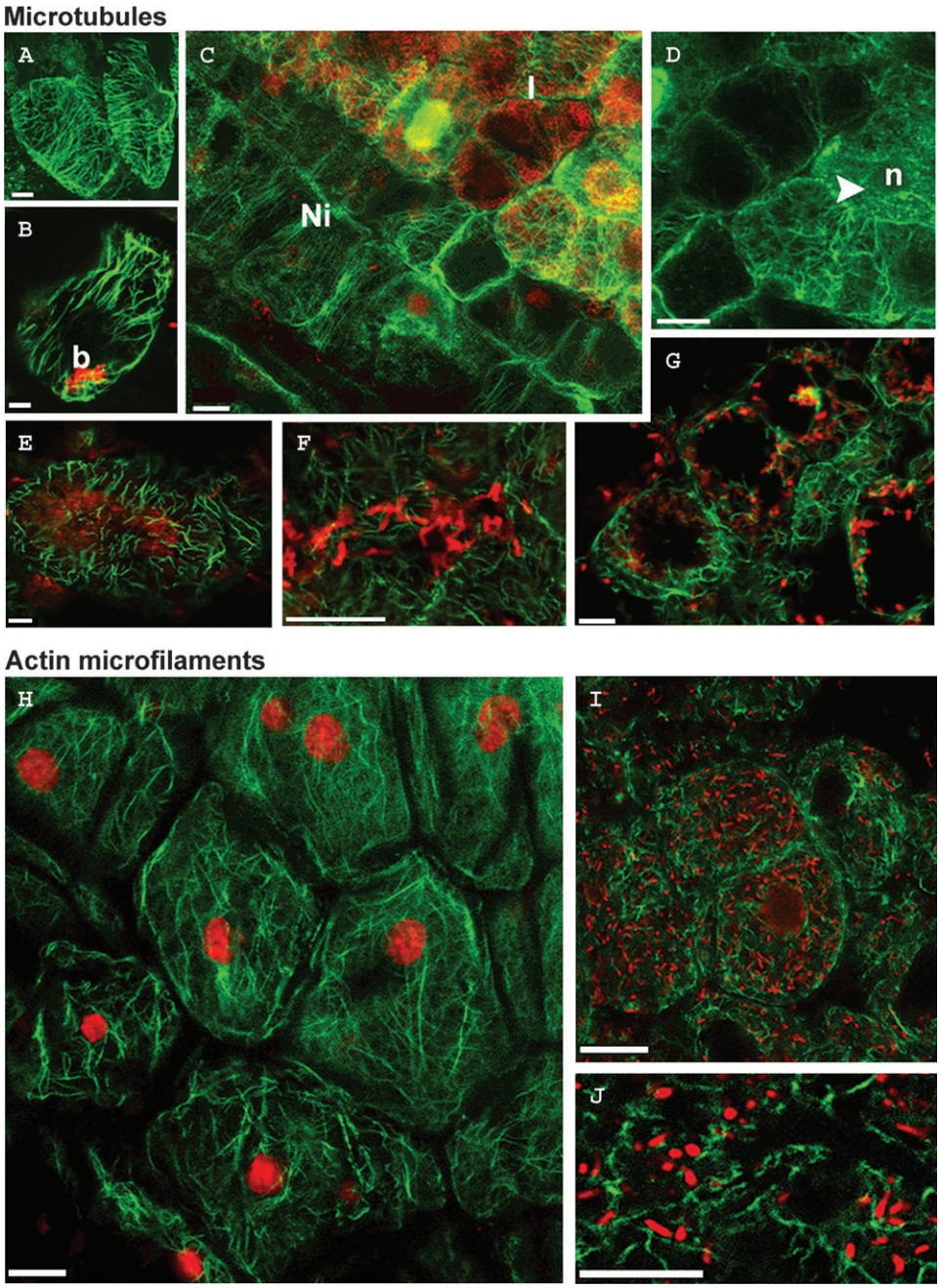

Fig. 2. Confocal laser microscope images (single optical sections except for F) of the interphase cell cytoskeleton in *Lupinus albus* nodules. Tubulin (A–G) and actin (H–J) were labelled green by using the secondary antibody IgG-Alexa 488 and Bodipy Pallacidin, respectively. Both probes emit a green fluorescence similar to that of fluorescein. Cells were counterstained with propidium iodide, which leaves DNA red. (A) Uninfected cortical cells. (B) Freshly infected cell containing several bacteroids (b). Note the alterations in the microtubules around the bacteroids. (C) Infected (I) and uninfected (Ni) cells. (D) Detail of C (red DNA labelling is omitted) showing long cortical microtubules and thin endoplasmic microtubule bundles randomly organized in a mature infected cell. Note the nucleus (n) surrounded by a perinuclear net (arrowhead). (E) Cortical microtubules in an infected cell. (F, G) Symbiosomes in contact with microtubules, (F) Z-stack combined, (G) single optical section. (H) Uninfected cortical cells. (I) Infected cells. (J) Symbiosomes in close contact with microfilaments. Bars: A, B, E=10 μm; C, D, I, J=50 μm; F, L=5 μm; G=16 μm.

(Fig. 3E, F), leading the cell plate towards the attachment sites. At this stage, the symbiosomes clustered behind the forming nuclei, already separated by the phragmoplast (Fig. 3F). The symbiosomes seemed to move coherently with the cytoplasm of the dividing cells, and were not seen in the midplane. At metaphase, anaphase, and early telophase, the symbiosomes were seen at the cell poles but not in the central zone (Fig. 3C–F). Cells undergoing asymmetrical division were frequently observed; the spindle and phragmoplast were not located in the central area but were confined to a more lateral position in the cell (Fig. 3G).

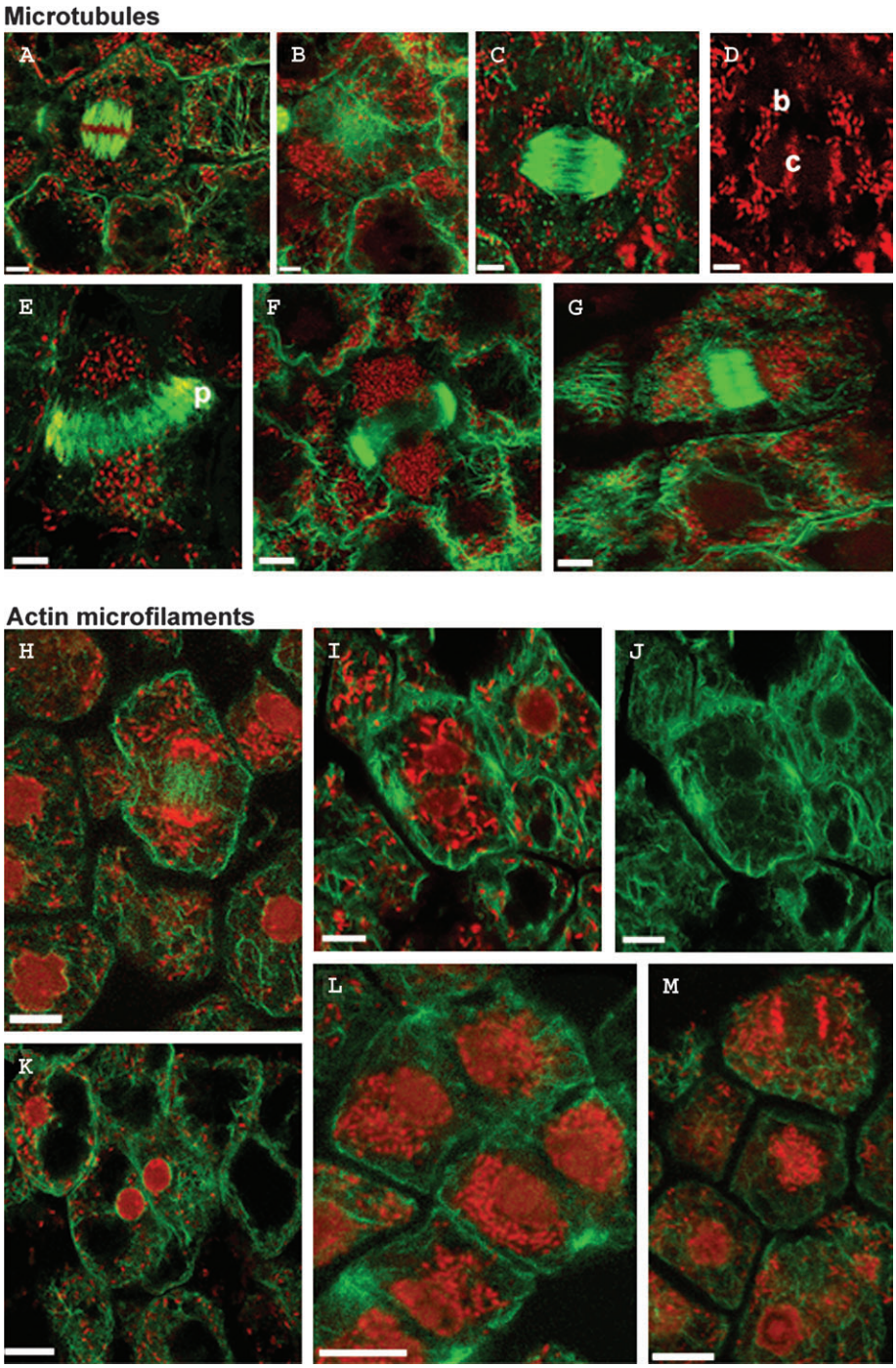

Fig. 3. Confocal laser microscope images (single optical sections except for B) of dividing infected cells of *Lupinus albus* nodules showing microtubules (A–G) or actin microfilaments (H–M) (green). DNA was labelled with propidium iodide (red). (A) Metaphase. Note that cortical strands are absent and only thin microtubule bundles can be seen in the cytoplasm. (B) Overlapping images from a Z-series of sections shown in A. (C, D) Anaphase. Separated chromatids (c) are pulled towards the poles; the bacteroids (b) are located in the lateral areas of the spindle and at the poles. (E, F) Late anaphase–early telophase. The phragmoplast (p) appears as a concentrated cylinder of microtubules between the daughter nuclei; the symbiosomes are symmetrically distributed behind the phragmoplast. (G) Asymmetrical division. (H) Metaphase. Microfilaments form the spindle. (I, J) Early telophase. (K) Late telophase. (L) Cells at different anaphase–telophase stages. Note the symbiosomes located behind the newly formed nuclei and opposite to the phragmoplast. (M) Asymmetrically dividing cell. Bars: A–D, H–J=10 μm; E–G, K–M=16 μm.

During cell division, the actin bundles in the cell cortex formed an extensive network. In the central zone of the cell the cytoplasmic actin strands were less visible; only spindle microfilaments were clearly detected (Fig. 3H). The symbiosomes did not interfere with the metaphase spindle but were mainly situated at the polar regions of

the cell, as during anaphase (Fig. 3I, J). In telophase, the cytoplasmic network of actin strands and the perinuclear network re-formed (Fig. 3I–K).

Once cytokinesis was complete in infected cells, the network of microtubules and microfilaments appeared to be completely re-established, and the symbiosomes migrated to the central and cortical regions of the cell (Fig. 3K). Bacterial division was not synchronized with host cell division; in fact, this was the only time when the bacteria were not dividing very actively. Eventually, however, the bacteria almost filled the cytoplasm of the host cell (Fig. 3L). This high degree of microsymbiont proliferation may have eventually affected the cell division pattern, leading to asymmetrically dividing cells (Fig. 3G, M).

Myosin-like protein in lupin nodules

To determine the possible presence of myosin in the lupin nodules, protein extracts from the nodules, root cytosol, and bacteroids were subjected to SDS-PAGE and western blot analysis using a monoclonal antibody against the myosin light chain (Fig. 4). The antibody immunorecognized several bands of approximately 20 kDa (the size expected for the myosin light chain) and 150 kDa in the root cytosol and nodule protein extracts. These larger polypeptides may represent partially degraded myosin heavy chains cross-reacting with the antibody. An additional band of approximately 65 kDa was immunodetected in the nodule extracts. The bacteroid extract gave no bands. The 65 kDa protein therefore appears to be a plant-specific protein, and is not a result of contamination with possible myosin-like proteins from the bacteroids.

The specificity of the immunodetection of the myosin antigen in the roots and nodules by the commercial anti-myosin light chain monoclonal antibody was estimated. After the depletion of the antibody with animal myosin light chain protein, no proteins were recognized in either the root or nodule extracts, nor was animal myosin detectable (western blotting) (Fig. 4C, D). This suggests that the antibody exclusively recognized myosin antigens in the lupin roots and nodules.

The immunolocalization of myosin-like protein (which is antigenically related to the light chain of animal myosin) in lupin nodules was performed by laser confocal (Fig. 5) and transmission electron (Fig. 6) microscopy. An intense immunofluorescent signal was observed in the cytosol, cell wall, and nucleoplasm of interphase infected cells (Fig. 5A, B). The immunolabelling pattern was diffuse compared with the filamentous pattern of actin labelling (Fig. 5A, B versus Fig. 2H, I). Intense fluorescence was seen in the perinuclear region in concordance with the actin network surrounding the nuclei (Fig. 5B, D). Similar labelling was also observed enveloping the nucleus of uninfected cells (Fig. 5C). In dividing infected cells, a fluorescent signal was also present over the spindle region (Fig. 5D). When the sister chromatids segregated,

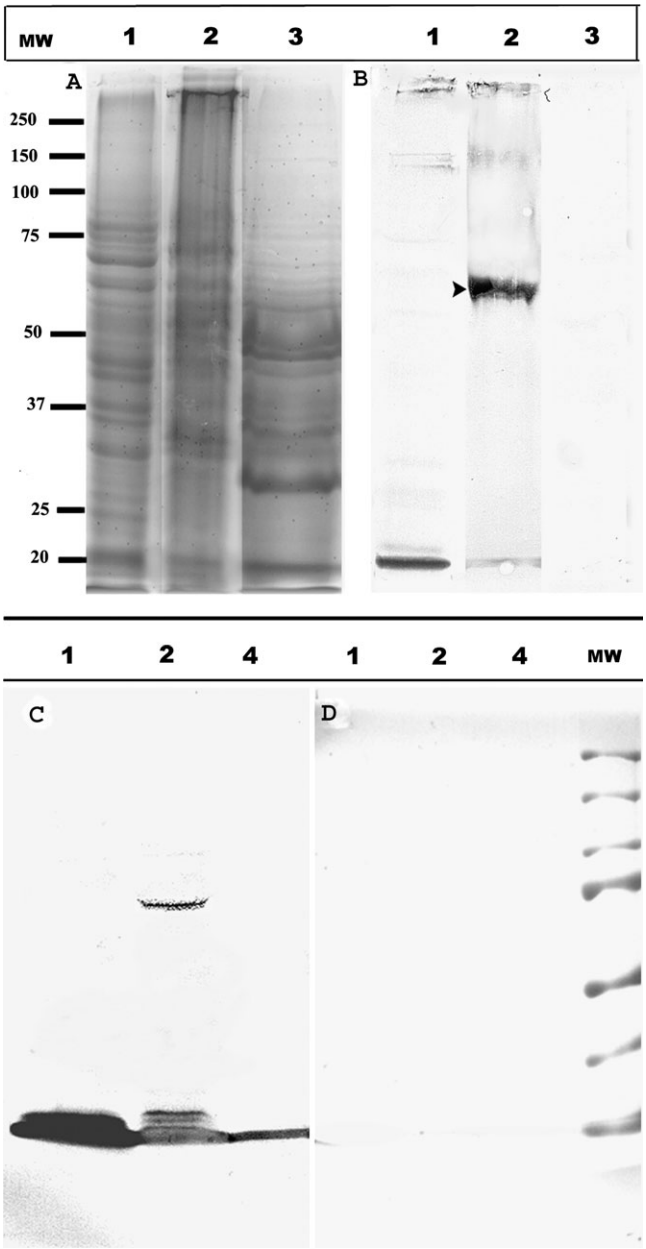

Fig. 4. SDS-PAGE (A) and western blot analysis of myosin light chain antigens in roots and nodules of *Lupinus albus* and in bacteroids. (B, C) Immunoblot with myosin light chain monoclonal antibody. (D) Immunoblot with the monoclonal antibody depleted by the light chain of animal myosin. Lane 1, cytosol of non-inoculated roots; 2, nodule cytosol; 3, bacteroid cytosol; 4, light chain of animal myosin.

the signal appeared between them. The myosin antigen signal appeared in a diffuse pattern opposite clear bundles of actin microfilaments in the spindle midzone (compare Figs 5D and 3H).

Electron microscopy confirmed the confocal microscopy results. Immunogold labelling revealed the cytosolic localization of the antigen (Fig. 6A). The nucleoplasm was intensely labelled; the signal was also observed in the perinuclear region (Fig. 6B). Immunogold particles were

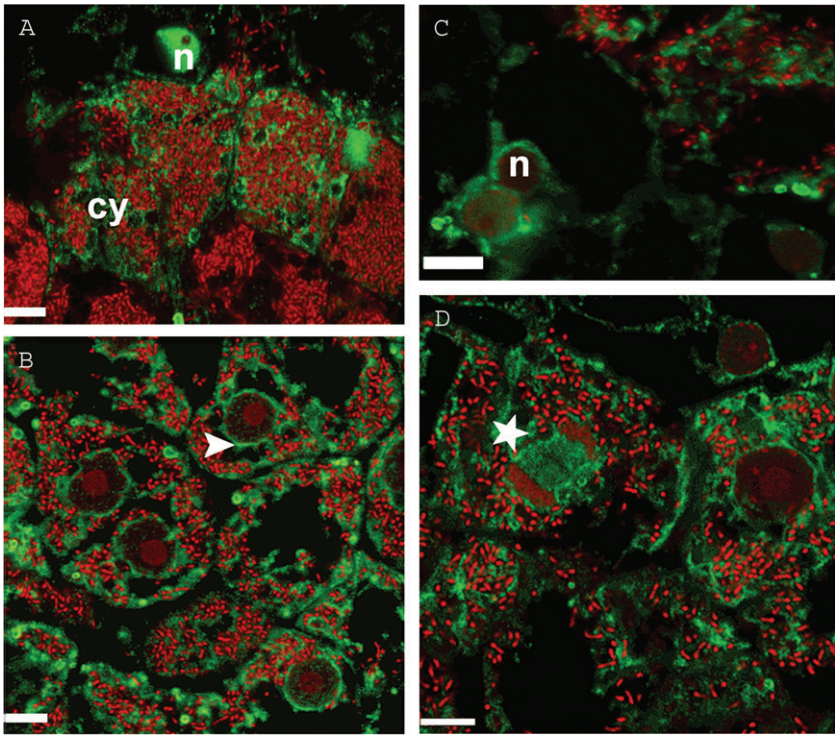

Fig. 5. Confocal laser microscope images (single optical sections) of *Lupinus albus* nodules labelled with anti-myosin light chain antibody (green) and propidium iodide (red). (A, B) Infected cells. Note the immunofluorescent signal in the cytosol (cy), nuclei (n), and perinuclear region (arrowheads) of infected cells. (C) Nuclei of non-infected cells. (D) Anaphase. Note the diffuse fluorescence in the spindle region (asterisk). Bars: A–D=10 μm.

seen over the thin microfilaments linked to the cell wall (Fig. 6C, D) and over the thicker microfilament bundles in the cell corners (Fig. 6E, F). The antibody also recognized epitopes located in cytoplasmic regions surrounding the symbiosomes (Fig. 6G–I), where they are probably associated with microfilaments in close contact with the symbiosome membranes. To confirm the presence of microfilaments in these regions, nodules with a better preserved ultrastructure (fixed in glutaraldehyde:paraformaldehyde and post-fixed with OsO_4; a treatment that does not allow immunolocalization) were analysed, and very thin filaments were clearly visible interacting with the symbiosomes (Fig. 6J).

Discussion

One of the key cellular events that occurs during legume nodulation is the reorganization of the plant cell cytoskeleton. The differences observed in different types of nodule suggest that cytoskeleton changes are symbiosis specific and rhizobia dependent (Timmers *et al*., 1998). Two main features differentiate *L. albus* nodules from other indeterminate and determinate nodules employed in cytoskeleton studies published to date. First, rhizobial infection of the root does not occur via infection threads; neither the nodule primordia nor the young nodules show these structures (James *et al*., 1997; González-Sama *et al*., 2004). Secondly, the cells remain able to divide after being infected (Tang *et al*., 1993; González-Sama *et al*., 2004), a lupinoid nodule feature that provides a suitable model for studying the division process of cells containing dividing prokaryotic organisms.

In infected lupin nodule cells in interphase, thick cortical arrays of microtubules appeared that formed a radial network of strands perpendicular to the cell wall. This is similar to that described by Timmers *et al*. (1998) in mature infected cells of alfalfa and siratro nodules. These authors proposed this pattern to facilitate the migration of organelles and symbiosomes to the periphery of the cells. In the present work, and again in lupin-infected nodule cells in interphase, actin was found forming wavy bundles connected to the nuclear-associated network, similar to that observed in soybean and pea nodules (Whitehead *et al*., 1998; Davidson and Newcomb, 2001*a*). It is plausible that the infected zone of both indeterminate and determinate nodules is composed of cells that enter interphase soon after being infected.

The presence of the microsymbiont in the cytoplasm of lupin nodule cells seems not to affect the latters' division. Such cells showed the normal microtubule pattern of a dividing plant cell (Wasteneys, 2002): endoplasmic, spindle, and phragmoplast microtubules were all present in metaphase and anaphase, although the cortical network was dissipated. In contrast to reports on *Medicago* nodules

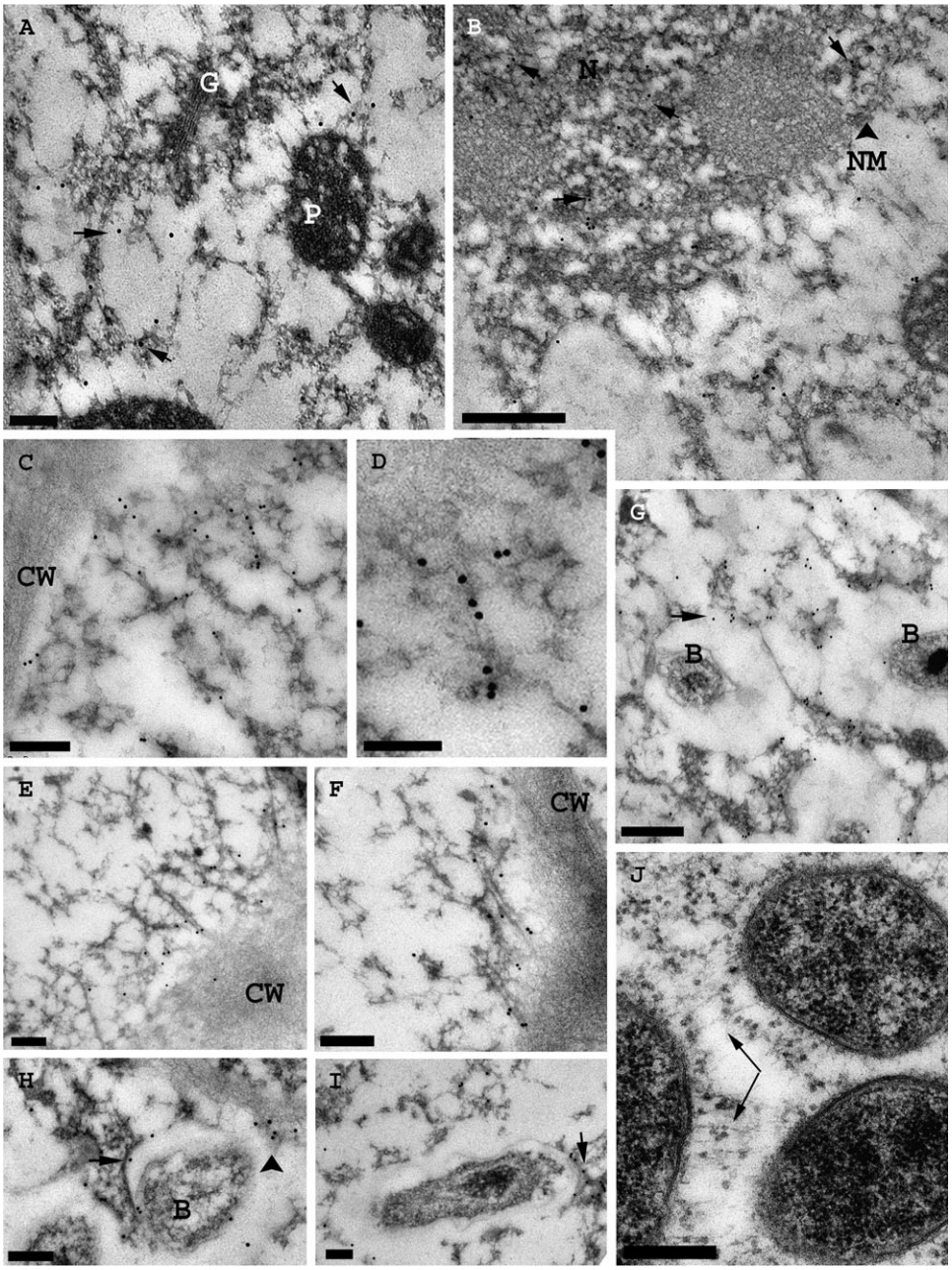

Fig. 6. Electron microscopy images showing immunogold localization of myosin in lupin nodules. (A) Gold particles (arrow) labelling cytosol epitopes. (B) Immunolabelling of nuclei. (C–F) Antigen localization in the cell wall region. (D) Magnification of (C), showing thin immunolabelled fibrils. (E, F) Gold particles on thick microfilament bundles. (G–I) Immunolabelled cytosol in the immediate vicinity of symbiosomes. Note the immunogold particles in the cell wall region in close contact with a symbiosome (arrowhead), and particles surrounding the symbiosome membrane (arrow). (J) Thin microfilaments (arrows) in close contact with symbiosome membranes in conventionally fixed nodules; this better preserves the ultrastructure than the fixation method used for immunocytochemistry. B, bacteroid; CW, cell wall; G, Golgi apparatus; P, plastid; N, nucleus; NM, nuclear membrane. Bars A, C, E, F, H–J=0.2 μm; B, G=0.5 μm; D=0.1 μm.

(Timmers *et al*., 1998, 1999), this dissipation appears to depend on cell cycle events and not on the fact that the cell has been infected. In agreement with the general actin pattern seen in dividing plant cells (Wasteneys and Galway, 2003), the cytoplasmic actin strands and the perinuclear microfilament envelope dissipated during metaphase–anaphase (when only the spindle microfilaments were present). The actin network was restored in late telophase. The changes in the microtubule and actin microfilament conformation in dividing infected lupin nodule cells should therefore be attributed to cell cycle events rather than to the presence of symbiosomes.

The present results provide new insight into how bacteroids are perceived by host cells. Lupin nodule cells

might recognize symbiosomes as their own cell organelles, at least when their number is low. Two observations strongly suggest this: the prokaryotes appear to be equally distributed between the daughter cells (González-Sama *et al*., 2004; this work), and the cytoskeleton conformation dynamics during the division of infected cells appear relatively normal. It may be that after several cell cycles the density of symbiosomes becomes so high that the host cell division mechanism becomes impaired. This could lead to the appearance of non-symmetrical division patterns and to abnormalities in the distribution of cytoskeletal elements that might prevent correct cytokinesis and, finally, the ability to divide.

The elaborate process of mitosis ensures that, during cytokinesis, each daughter cell receives a full set of chromosomes together with a proper complement of cytoplasm and organelles. The mechanisms that regulate this organelle distribution may also be involved in symbiosome segregation.

Endosymbiotic rhizobia do not come into direct contact with the host cell cytoplasm because of the symbiosome membrane. This is initially formed of host cell plasma membrane picked up during endocytosis, but later appears as a hybrid or mosaic of the plasma membrane and tonoplast (Roth and Stacey, 1989). It also harbours proteins derived from the bacteroid (Catalano *et al*., 2004). Certain similarities with the movement and segregation of provacuole clusters [found in the polar regions of dividing plant cells (Marty, 1999)] and symbiosomes may be expected due to the tonoplast features of the peribacteroid membrane. It is likely that symbiosome movement and segregation rely on the same mechanisms involved in the positioning of Golgi bodies and provacuoles, which, in plants, depend mainly on the actin–myosin system (Nebenführ *et al*., 1999, 2000; Shimmen and Yokota, 2004).

In plant cells, myosin is believed to participate as a motor in the intracellular transport of organelles and vesicles, referred to as cytoplasmic streaming (Reddy, 2001). Several studies suggest that the movement and positioning of chloroplasts (Takagi, 2003), peroxisomes (Jedd and Chua, 2002; Mathur *et al*., 2002), mitochondria, and Golgi bodies (Nebenführ *et al*., 1999; Van Gestel *et al*., 2002) are regulated by actin configuration and myosin motors. Phylogenetic analyses have shown that most of the plant myosins discovered to date belong to either class VIII or class XI (Reddy 2001; Wasteneys and Galway, 2003). Imunolocalization of the myosin heavy chain in the roots of *Allium cepa*, *Zea mays*, and *Hordeum vulgare* resulted in labelling over the plasmodesmata, the plasma membrane, the cytosol, and vesicles or small organelles (Radford and White, 1998; Samaj *et al*., 2000; Liu *et al*., 2001). More recently, a subclass XI myosin has been shown associated with mitochondria and plastids (Wang and Pasacreta, 2004).

In lupin nodule cells, the myosin light chain antigen was detected in the cytoplasm and the perinuclear region, spatially co-localizing with actin bundles. Specific immunolabelling of microfilament bundles connected with the cell wall and the cytoplasmic areas surrounding the symbiotic organelles (symbiosomes) was detected by electron microscopy. In animal cells, myosin also co-localizes with actin filament bundles and is found in the perinuclear region (Sakurada *et al*., 1998; Bryce *et al*., 2003). The significance of the different localizations seen in this work compared with the immunolocalization of other myosin proteins in plant cells should be investigated. The isolation and characterization of the myosin-like protein antigens in lupin nodules, and the immunolocalization of myosin class VIII and class XI in nodules, are the goals of future work.

In all dividing eukaryotic cells, the clustered organelles tethered to the spindle-pole regions move to the cell poles during spindle elongation using cytoskeleton elements and molecular motors. This ensures organelle inheritance. The symmetric distribution of symbiosomes in metaphase–anaphase infected cells, the close contact of symbiosomes with cytoskeletal elements, and the presence of myosin-like antigen in infected cells suggest that the segregation of symbiosomes during host cell division in lupin nodules might be driven by a similar mechanism.

Acknowledgements

The authors thank Dr Barasoain for his help with methods of tubulin staining, MC Hernández Capitán for technical assistance with the laser confocal microscope, and F Pinto for technical assistance with the transmission electron microscope. This work was supported by grants BIO2001-2355 and AGL2001-2093 from the Ministerio de Ciencia y Tecnología (MCYT) (Spain). EEF was a recipient of an MCYT sabbatical contract.

References

Allen NS, Bennett MN, Cox DN, Shipley A, Ehrhardt DW, Long SR. 1994. Effects of Nod factors on alfalfa root hair Ca^{++} and H^{+} currents and on cytoskeletal behaviour. In: Daniels MJ, Downie JA, Osbourn AE, eds. *Advances in molecular genetics of plant–microbe interactions*, Vol. III. Dordrecht, The Netherlands: Kluwer Academic Publishers, 107–113.

Bergersen FJ. 1982. Anatomy and structure of nodules. In: *Root nodule of legumes: structure and functions*. Baldock, UK: Research Studies Press, 23–50.

Brewin NJ. 1991. Development of the legume root nodule. *Annual Review of Cell Biology* **7,** 191–226.

Brewin NJ, Robertson JG, Wood EA, Wells B, Larkins AP, Galfre G, Butcher GW. 1985. Monoclonal antibodies to antigens in the peribacteroid membrane from *Rhizobium*-induced root nodules of pea cross-react with plasma membranes and Golgi bodies. *EMBO Journal* **4,** 605–611.

Bryce NS, Schevzov G, Ferguson V, *et al*. 2003. Specification of actin filament function and molecular composition by tropomyosin isoforms. *Molecular Biology of the Cell* **14,** 1002–1016.

Cárdenas L, Thomas-Oates JE, Nava N, López-Lara IM, Kepler PK, Quinto C. 2003. The role of Nod factor substituents in actin cytoskeleton rearrangements in *Phaseolus vulgaris*. *Molecular Plant–Microbe Interactions* **16,** 326–334.

Cárdenas L, Vidali L, Domínguez J, Pérez H, Sánchez F, Hepler PK, Quinto C. 1998. Rearrangement of actin microfilaments in plant root hairs responding to *Rhizobium etli* nodulation signals. *Plant Physiology* **116,** 871–877.

Catalano CM, Lane WS, Sherrier DJ. 2004. Biochemical characterization of symbiosome membrane proteins from *Medicago truncatula* root nodules. *Electrophoresis* **25,** 519–531.

Chandler MR. 1978. Some observations on infected nodules of *Arachis hypogea* L. by *Rhizobium*. *Journal of Experimental Botany* **29,** 749–755.

Chandler MR, Date RA, Roughley RJ. 1982. Infection and root-nodule development in *Stylosanthes* species by *Rhizobium*. *Journal of Experimental Botany* **33,** 47–57.

Davidson AL, Newcomb W. 2001*a*. Changes in actin microfilament arrays in developing pea root nodule cells. *Canadian Journal of Botany* **79,** 767–776.

Davidson AL, Newcomb W. 2001*b*. Organization of microtubules in developing pea root nodule cells. *Canadian Journal of Botany* **79,** 777–786.

Drøbak BK, Franklin-Tong VE, Staiger CJ. 2003. The role of the actin cytoskeleton in plant cell signalling. *New Phytologist* **163,** 13–30.

Douglas SE. 1998. Plastid evolution: origins, diversity, trends. *Current Opinion in Genetic Development* **8,** 655–661.

Fedorova E, Thomson R, Whitehead LF, Maudoux O, Udvardi MK, Day DA. 1999. Localization of H^+-ATPase in soybean root nodules. *Planta* **209,** 25–32.

Fedorova E, Redondo FJ, Koshiba T, de Felipe MR, Pueyo JJ, Lucas MM. 2005. Aldehyde oxidase (AO) in the root nodules of *Lupinus albus* and *Medicago truncatula*: identification of AO in meristematic and infection zones. *Molecular Plant–Microbe Interactions* **18,** 405–413.

González-Sama A, Lucas MM, de Felipe MR, Pueyo JJ. 2004. An unusual infection mechanism and nodule morphogenesis in white lupin (*Lupinus albus*). *New Phytologist* **163,** 371–380.

González-Sama A, Coba de la Peña T, Kevei Z, Mergaert P, Lucas MM, de Felipe MR, Kondorosi E, Pueyo JJ. 2006. Nuclear DNA endoreduplication and expression of the mitotic inhibitor Ccs52 associated to determinate and lupinoid nodule organogenesis. *Molecular Plant–Microbe Interactions* **19,** 173–180.

Gray MW, Burger G, Lang BF. 1999. Mitochondrial evolution. *Science* **283,** 1476–1481.

Hashimoto T. 2003. Dynamics and regulation of plant interphase microtubules: a comparative view. *Current Opinion in Plant Biology* **6,** 568–576.

James EK, Minchin FR, Iannetta PPM, Sprent JI. 1997. Temporal relationships between nitrogenase and intercellular glycoprotein in developing white lupin nodules. *Annals of Botany* **79,** 493–503.

Jedd G, Chua N-H. 2002. Visualization of peroxisomes in living plant cells reveals actomyosin-dependent cytoplasmic streaming and peroxisome budding. *Plant Cell Physiology* **43,** 384–392.

Kalita M, Stepkowski T, Lotocka B, Malek W. 2006. Phylogeny of nodulation genes and symbiotic properties of *Genista tinctoria* bradyrhizobia. *Archives of Microbiology* **186,** 87–97.

King SM. 2002. Dyneins motor on in plants. *Traffic* **3,** 930–931.

Lhuissier FGP, De Ruijter NCA, Sieberer BJ, Esseling JJ, Emons AMC. 2001. Time course of cell biological events evoked in legume root hairs by *Rhizobium* Nod factors: state of the art. *Annals of Botany* **87,** 289–302.

Liu LY, Zhou JH, Pesacreta TC. 2001. Maize myosins: diversity, localization and function. *Cell Motility and the Cytoskeleton* **48,** 130–148.

Lodwig EM, Hosie AH, Bourdes A, Findlay K, Allaway D, Karunakaran R, Downie JA, Poole PS. 2003. Amino-acid cyling drives nitrogen fixation in the legume–*Rhizobium* symbiosis. *Nature* **422,** 722–726.

Marty F. 1999. Plant vacuoles. *The Plant Cell* **11,** 587–599.

Mathur J, Mathur N, Hülskamp M. 2002. Simultaneous visualization of peroxisomes and cytoskeletal elements reveals actin and not microtubule-based peroxisome motility in plants. *Plant Physiology* **128,** 1031–1045.

Nebenführ A, Gallagher OA, Dunahay TG, Frohlick JA, Mazurkiewics AM, Meehl JB, Stahelin LA. 1999. Stop-and-go movements of plant Golgi stacks are mediated by the actomyosin system. *Plant Physiology* **121,** 1127–1141.

Nebenführ A, Frohlick JA, Staehelin LA. 2000. Redistribution of Golgi stacks and other organelles during mitosis and cytokinesis in plant cells. *Plant Physiology* **124,** 135–152.

Parniske M. 2000. Intracellular accommodation of microbes by plants: a common developmental program for symbiosis and disease? *Current Opinion in Plant Biology* **3,** 320–328.

Patriarca EJ, Taté R, Fedorova E, Riccio A, Defez R, Iaccarino M. 1996. Down-regulation of the *Rhizobium ntr* system in the determinate nodule of *Phaseolus vulgaris* identifies a specific developmental zone. *Molecular Plant–Microbe Interactions* **9,** 243–251.

Patriarca EJ, Taté R, Ferraioli S, Iaccarino M. 2004. Organogenesis of the legume root nodules. *International Review of Cytology* **234,** 201–262.

Radford JR, White RJ. 1998. Localization of myosin-like protein to plasmodesmata. *The Plant Journal* **14,** 743–750.

Reddy ASN. 2001. Molecular motors and their functions in plants. *International Review of Cytology* **204,** 97–178.

Roth LE, Stacey G. 1989. Bacterium release into host cell of nitrogen-fixing soybean nodules: the symbiosome membrane comes from three sources. *European Journal of Cell Biology* **49,** 13–23.

Sajnaga E, Malek W, Lotocka B, Stepkowski T, Legocki A. 2001. The root-nodule symbiosis between *Sarothamnus scoparius* L. and its microsymbionts. *Antonie van Leewenhoek* **79,** 385–391.

Sakurada K, Seto M, Sasaki Y. 1998. Dynamics of myosin light chain phosphorylation at Ser19 and Thr18/Ser19 in smooth muscle cells in culture. *American Journal of Physiology* **274,** C1563–C1572.

Samaj J, Peters M, Volkmann D, Baluska F. 2000. Effects of myosin ATPase inhibitor 2,3 butanedione 2-monoxime on the distribution of myosins, F-actin, microtubules and cortical endoplasmic reticulum in maize root apices. *Plant and Cell Physiology* **41,** 571–582.

Sheahan MB, Rose RJ, McCurdy DW. 2004. Organelle inheritance in plant cell division: the actin cytoskeleton is required for unbiased inheritance of chloroplasts, mitochondria and endoplasmic reticulum in dividing protoplasts. *The Plant Journal* **37,** 379–390.

Shimmen T, Yokota E. 2004. Cytoplasmic streaming in plants. *Current Opinion in Cell Biology* **16,** 68–72.

Sieberer BJ, Timmers ACJ, Emons AM. 2005. Nod factors alter the microtubule cytoskeleton in *Medicago truncatula* root hairs to allow root hair reorientation. *Molecular Plant–Microbe Interactions* **18,** 1195–1204.

Takagi S. 2003. Actin-based photo-orientation movement of chloroplasts in plant cells. *Journal of Experimental Biology* **54,** 1963–1969.

Takemoto D, Hardham AR. 2004. The cytoskeleton as a regulator and target of biotic interactions in plants. *Plant Physiology* **136,** 3864–3876.

Tang C, Robson AD, Kuo J, Dilworth MJ. 1993. Anatomical and ultrastructural observations on infection of *Lupinus angustifolius* L by *Bradyrhizobium* sp. *Journal of Computer-Assisted Microscopy* **5,** 47–51.

Timmers ACJ, Auriac M-C, de Billy F, Truchet G. 1998. Nod factor internalisation and microtubular cytoskeleton changes occur concomitantly during nodule differentiation in alfalfa. *Development* **125,** 339–349.

Timmers ACJ, Auriac M-C, Truchet G. 1999. Refined analysis of early symbiotic steps of the *Rhizobium–Medicago* interaction in relationship with microtubular cytoskeleton rearrangements. *Development* **126,** 3617–3628.

Van Gestel K, Köhler RH, Verbelen J-P. 2002. Plant mitochondria move on F-actin, but their positioning in the cortical cytoplasm depends on both F-actin and microtubules. *Journal of Experimental Botanty* **53,** 659–667.

Vassileva VN, Kouchi H, Ridge RW. 2005. Microtubule dynamics in living root hairs: transient slowing by lipochitin oligossacharide nodulation signals. *The Plant Cell* **17,** 1777–1787.

Wang Z, Pasacreta TC. 2004. A subclass of myosin XI is associated with mitochondria, plastids, and molecular chaperone subunit TCP-1alpha in maize. *Cell Motility and the Cytoskeleton* **57,** 218–232.

Warren G, Wickner W. 1996. Organelle inheritance. *Cell* **84,** 395–400.

Wasteneys GO. 2002. Microtubule organization in the green kingdom: chaos or self-order? *Journal of Cell Science* **115,** 1345–1354.

Wasteneys GO, Galway ME. 2003. Remodeling the cytoskeleton for growth and form. An overview with some new views. *Annual Review of Plant Biology* **54,** 691–722.

Weeransinghe RR, Collings DA, Johannes E, Allen NS. 2003. The distributional changes and role of microtubules in Nod factor-challenged *Medicago sativa* root hairs. *Planta* **218,** 276–287.

Whitehead LF, Day DA, Hardham AR. 1998. Cytoskeleton arrays in the cells of soybean root nodules: the role of actin microfilaments in the organisation of symbiosomes. *Protoplasma* **203,** 194–205.